Astronomy & Astrophysics manuscript no. 17434˙accepted
January 4, 2012

© ESO 2012

arXiv:1201.0439v1 [astro-ph.CO] 2 Jan 2012

The ancient stellar population of M 32: RR Lyr Variable stars confirmed

G. Fiorentino[1], R. Contreras Ramos[2], E. Tolstoy[3], G. Clementini[1], A. Saha[4]

[1] INAF-Osservatorio Astronomico di Bologna, via Ranzani 1, 40127, Bologna e-mail: `giuliana.fiorentino@oabo.inaf.it`
[2] Dipartimento di Astronomia, Universitá degli studi di Bologna, via Ranzani 1, 40127, Bologna
[3] Kapteyn Astronomical Institute, University of Groningen, Groningen, The Netherlands
[4] NOAO, P.O. Box 26732, Tucson, AZ 85726, US

Received June 9, 2011; accepted Dec 15, 2011

ABSTRACT

Using archival multi–epoch ACS/WFC images in the F606W and F814W filters of a resolved stellar field in Local Group dwarf elliptical galaxy M 32 we have made an accurate Colour−Magnitude Diagram and a careful search for RR Lyr variable stars. We identified 416 bona fide RR Lyr stars over our field of view, and their spatial distribution shows a rising number density towards the centre of M 32. These new observations clearly confirm the tentative result of Fiorentino et al. (2010), on a much smaller field of view, associating an ancient population of RR Lyr variables to M 32. We associate at least 83 RR Lyr stars in our field to M 32.

In addition the detection of 4 Anomalous Cepheids with masses in the range 1.2−1.9 $M_\odot$ indicates the presence of relatively young, 1−4 Gyr old, stars in this field. They are most likely associated to the presence of the blue plume in the Colour−Magnitude Diagram. However these young stars are unlikely to be associated with M 32 because the radial distribution of the blue plume does not follow the M 32 density profile, and thus they are more likely to belong to the underlying M 31 stellar population. Finally the detection of 3 Population II Cepheids in this field gives an independent measurement of the distance modulus in good agreement with that obtained from the RR Lyr, μ_0=24.33 ± 0.21 mag.

Key words. Local Group — galaxies: individual: M 32, M 31 — stars: horizontal-branch – stars: variables: other

1. Introduction

The compact dwarf elliptical galaxy M 32 is one of the few elliptical galaxies close enough that, with the help of HST, direct observations can be made of its ancient resolved stellar population (e.g., Grillmair et al. 1996; Alonso-García et al. 2004; Fiorentino et al. 2010b; Monachesi et al. 2011). Another example is the peculiar giant elliptical galaxy Cen A, at a distance of 3.8 Mpc, where the red giant branch (RGB) and red clump (RC) have been resolved in the outer halo (e.g., Rejkuba et al. 2011). More distant elliptical galaxies, and also the extremely high surface brightness inner regions of M 32, can only be studied in integrated light (e.g., Renzini 2006; Rose 1994; Trager et al. 2000; Coelho et al. 2009). Integrated light provides a picture of the mean properties of a galaxy, but these analyses are rarely unique and cannot avoid a strong bias from the dominant stellar population.

The search for traces of an old (>10 Gyr) stellar population is the main motivation for this study of the resolved stellar population of M 32. RRLyr variable stars are unequivocal indicators of the presence of a stellar population > 10 Gyr old. There have been a number of detailed studies of the RRLyr population of M 31, both with ground−based wide field surveys of the halo (Pritchet & van den Bergh 1987; Dolphin et al. 2004), and HST monitoring of M 31 globular clusters (Clementini et al. 2009) and small halo and disk fields (Brown et al. 2004; Jeffery et al. 2011). Thare have also been studies in the region around M 32 (Alonso-García et al. 2004; Sarajedini et al. 2009; Fiorentino et al. 2010b).

A recent analysis of the resolved stellar population of M 32 using the ACS/HRC camera, which has a tiny field of view ∼ 30x30 arsec square (see small blue square in Fig. 1) but very high spatial resolution (a factor two better than WFC/ACS), concluded that the bulk of the stellar population has an age in the range 8 − 10 Gyrs old, with a mean metallicity, [Fe/H]∼ −0.2 dex (Monachesi et al. 2011). However their Colour-Magnitude-Diagram (CMD) did not reach the Main Sequence Turn Off stars of the oldest stellar population. They also associated a faint blue plume (BP) of stars in the CMD to ≥1 Gyr old stars in M 32. Using the same ACS/HRS data 17 RRLyr were found, and it was tentatively suggested that 7^{+4}_{-3} could be associated to M 32 (Fiorentino et al. 2010b). The small field of view made this result highly uncertain simply due to the poor spatial sampling of a sparse population and the significant contamination from M 31. Here we use archival ACS/WFC data, with significantly better spatial coverage (see large red square in Fig. 1), to revisit the detection of RRLyr associated with M 32.

2. Data reduction and analysis

We used 36 archival ACS/WFC images[1], covering a 3.3 x 3.3 arcmin square region, centred at 00 42 56 +40 50 50 (J2000), and extending from 1 to 4.5 arcmin from the centre of M 32, see Fig. 1 and Table 1. The cadence of the images was chosen with the aim of picking up short period variable stars (periods <1 day), which includes RRLyr. The sensitivity of the temporal sampling to these short periods is close to ∼100% complete, for variable stars with periods <1 day.

---

[1] Proposal id: 9392; PI: M. Mateo

Table 1. Log of the M 32 ACS/WFC archival data.

Field	$\alpha_{J2000.0}$	$\delta_{J2000.0}$	Filter	Exposure time	Date
F1	$00^h42^m56^s$	+40°50′50″	*F*606*W*	8×1000	24 Nov 2004
F1	$00^h42^m56^s$	+40°50′50″	*F*606*W*	5×1000	25 Nov 2004
F1	$00^h42^m56^s$	+40°50′50″	*F*606*W*	5×1000	10 Dec 2004
F1	$00^h42^m56^s$	+40°50′27″	*F*814*W*	8×1580	24 Nov 2004
F1	$00^h42^m56^s$	+40°50′27″	*F*814*W*	5×1580	25 Nov 2004
F1	$00^h42^m56^s$	+40°50′27″	*F*814*W*	5×1580	10 Dec 2004

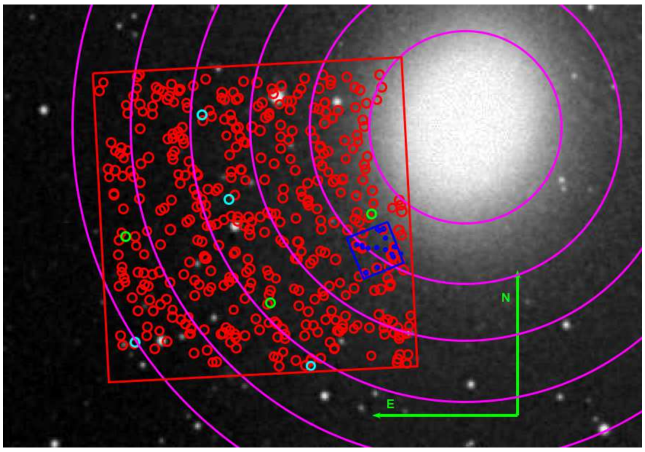

Fig. 1. A 6 x 5 arcmin DSS2 where our ACS/WFC field is shown as a large (red) square. The HRC field with its RRLyr (from Fiorentino et al. 2010b) is shown as a small (blue) square. The RRLyr, Anomalous Cepheid and Population II Cepheid variables detected in the ACS/WFC field are shown as red, cyan and green points, respectively. Circles centred on M 32 used in the density analysis are plotted in magenta.

2.1. Photometric analysis

We used the same data reduction and analysis techniques described in Fiorentino et al. (2010a,b). The PSF−fitting photometry was carried out using DOLPHOT, a version of HSTphot modified for ACS images (Dolphin 2000b). DOLPHOT returns a time series of measurements for each image as well as a final mean magnitude for all stars found on all the individual frames. DOLPHOT also makes automatic aperture corrections, following the prescription of Sirianni et al. (2005), and corrects for charge transport efficiency (CTE) effects (as described in Dolphin 2000a). Thus we end up with a final catalogue consisting of a time series of 18 individual photometric measurements in two filters, plus mean magnitudes, for ∼400 000 stars over the entire ACS/WFC field of view.

There is clearly a very strong gradient in stellar density across our field of view, which increases towards the centre of M 32. This gradient leads to large variations in the crowding of the stellar images. We thus also performed artificial star tests to quantify the completeness of the photometric catalogue over the field of view. A mean completeness above 90% for the whole field is only found for stars with $m_{F606W} \leq 24.5$ mag. For stars fainter than this, the completeness drops rapidly towards the centre of M 32, as the stellar density increases. This has to be carefully corrected before conclusions can be drawn about grandients across this field. We come back to this point in Section 5.

We also tested our photometric catalogue for evidence of differential reddening across the field using the well established method of Piotto et al. (1999). We divided our field into 64 26x26 arcsec^2 regions and selected one of these as reference. Then for each sub-region we compared the CMD properties with the reference. No evidence for differential reddening was found, down to a limit of m_{F606W} = 26 mag, and thus we adopted a single reddening value of E(B−V) = 0.08 mag (A_{F606W}=0.21 mag, A_{F814W}=0.13 mag, see Fiorentino et al. 2010b; Bedin et al. 2005), in our analysis.

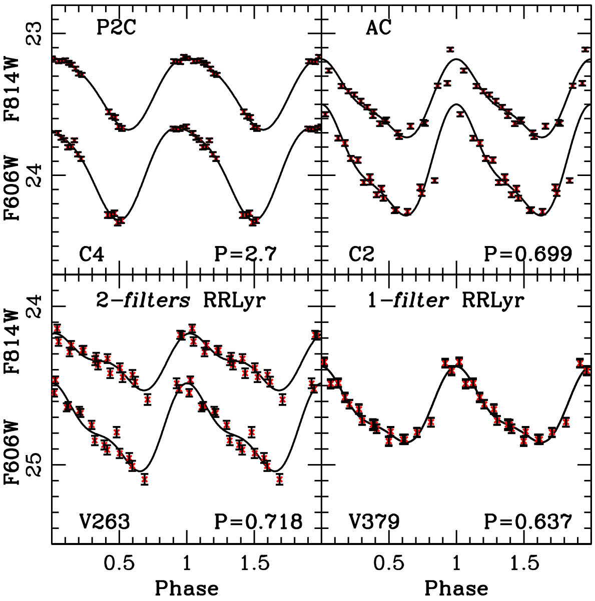

Fig. 2. An example of the quality of the light curves in F606W and F814W filters for four detected variable stars, a Population II Cepheid, an Anomalous Cepheid, a *one-filter* and a *two-filters* RRLyr. The ID, type and period have been labeled. The fitting model used to determine the mean magnitude and amplitude has been overplotted. The errorbars represent the photometric error returned by DOLPHOT.

2.2. Search for variability

Details of the procedures to detect and classify variable stars are described in Fiorentino et al. (2010b). The average errors on the periods are < 0.01 day, on the amplitudes of the variation are < 0.1 mag and on the mean magnitudes are < 0.1 mag. We identified 416 bona–fide RRLyr. We divided the RRLyr into two groups, *two-filters* (351 RRLyr) and *one-filter* (65 RRLyr). For *two-filters* candidates we were able to properly phase the F606W and F814W light curves. For the *one-filter* candidates we could estimate the period using only one filter (usually F606W). We identified also 4 Anomalous Cepheids (AC) and 3 Population II Cepheids (P2C), see Section 4. In Fig. 2 we show the light curves we have obtained for 2 RRLyr, 1 AC and 1 P2C. We have also detected 61 variable candidates which cannot be accurately

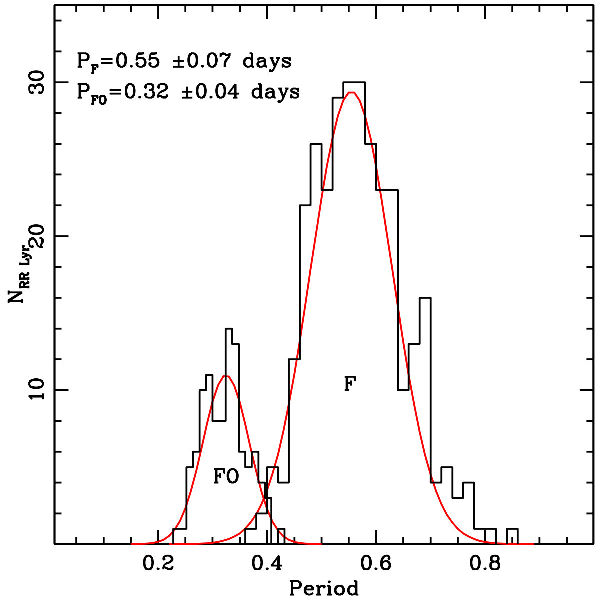

Fig. 3. The period distributions of the fundamental (right) and first-overtone (left) RRLyr. The periods corresponding to the gaussian (red) peaks are given as P_F and P_{FO}.

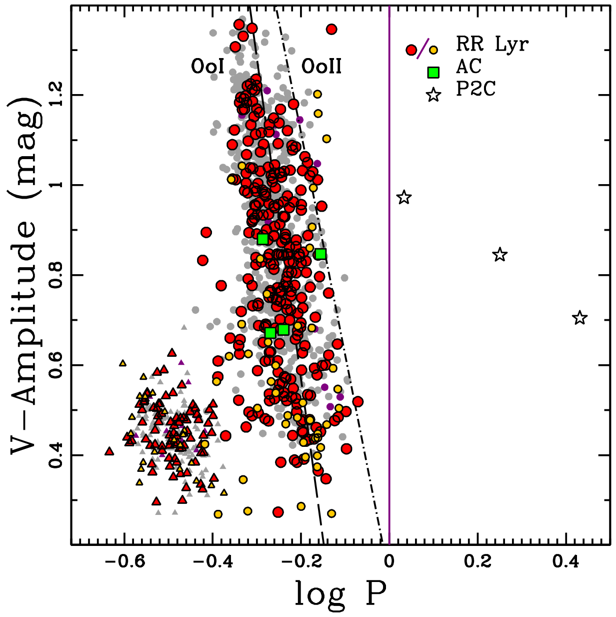

Fig. 4. The V filter amplitude – period (P) Bailey diagram for our observations (coloured symbols) and the observations of M 31 RRLyr from Sarajedini et al. (2009) and Brown et al. (2004) as grey and magenta symbols. The Oosterhoff type loci, OoI (dashed) and OoII (dot−dashed), are shown (from Clement 2000). For the RRLyr the triangles are first-overtone pulsators and the circles are fundamental pulsators. RRLyr *two-filters* are plotted in red and only in *one-filter* in orange. Anomalous Cepheids and Population II Cepheids are indicated with squares (green) and stars, respectively.

classified, they include 27 possible RRLyr and 34 longer period variables.

We have recovered 9 of the 17 RRLyr (~ 53 %) found in our previous study with ACS/HRC (Fiorentino et al. 2010b), confirming the low mean completeness (~ 57 %) of the HB luminosity on the present ACS/WFC images so close to M 32.

3. The RRLyr variable stars

From the 416 bona− fide RRLyr we have detected, we classify 314 as fundamental pulsators (F or RR_{ab}) and 102 first−overtone pulsators (FO or RR_c). Table 2 lists the RRLyr along with their properties such as position, period, pulsation type classification, mean intensity−weighted magnitudes, amplitudes and de−reddened mean magnitudes transformed in the Johnson−Cousin photometric system. The RR Lyrae have been named using their increasing distance from the centre of M 32.

The mean period distribution of the F pulsators matches a gaussian peaked at P_F =0.55 days with σ = 0.07 days, see Fig. 3, which is consistent with Oosterhoff type I. Similarly, a mean period of P_{FO} = 0.32 days with σ = 0.04 days is found for FO pulsators, which is also consistent with an Oosterhoff type I. The ratio between the number of FO and the total sample, N_{FO}/N_{TOT} ~ 0.25. Our results are thus in agreement with the M 31 study performed by Sarajedini et al. (2009) of two ACS fields close to M 32. Other deep HST/ACS observations of RRLyr M 31 include six fields of the halo, disk, and giant stellar stream have been studied by Jeffery et al. (2011). The RRLyr of these fields appear to mostly be of Oosterhoff I type. Comparing our results with these six M 31 fields which sample different components of M 31, the properties of our sample resembles the giant stream of M 31, where they found $< P_F >$=0.56 and N_{FO}/N_{TOT}=0.33.

3.1. Bailey diagram and metallicity

Fig. 4 shows the Bailey diagram of the variable stars detected in the present study overlaid on the M 31 studies of Sarajedini et al. (2009); Brown et al. (2004). This diagram divides into two regions, at log P=0, to distinguish the variable star types. At log P< 0 are the RRLyr and AC and at log P> 0 the P2C. The $F606W$ amplitudes have been transformed to V−filter amplitudes (Brown et al. 2004) using A_{F606W}=92 % A_V to directly compare the Oosterhoff (Oo) type loci (see Clement 2000, and references therein). In Fig. 4 we see that F RRLyr are predominantly consistent with an Oo type I, confirming the Oo classification based on the periods alone.

Next, we use this V amplitude−period relation (given by Alcock et al. 2000) to determine the individual metallicities of our entire sample of RRLyr. This is a method commonly used in the literature for RRLyr studies without colour information. We found a mean metallicity [Fe/H]=−1.44±0.55 dex for our sample, comparable with what was found in M 31. Sarajedini et al. (2009) found [Fe/H] = −1.45±0.45 for their F1 field (the closest to M 32) and [Fe/H] = −1.54±0.43 for their F2. In Fig. 5 we show a comparison between individual metallicities for our sample and Sarajedini's sample. We can see that our results are in very good agreement with their studies. We also notice that in our field, and also in the Sarajedini field closest to M 32, there are a few RRLyr of solar metallicity. This means that we observe more metal−rich RRLyr than have been found in the halo, disk and giant stream of M 31 by Brown et al. (2004) and Jeffery et al. (2011), where using the same method, no RRLyr with metallicity larger than [Fe/H] >−1 dex have been found.

Table 2. The RRLyr variable stars we have identified. The mean F606W and F814W magnitudes are intensity−weighted over the light curve. V_0 and I_0 are the de−reddened mean magnitudes in the Johnson−Cousin photometric system obtained following the prescriptions by Sirianni et al. (2005). Type classification, RR_{ab} and RR_c, indicate fundamental and first−overtone pulsation modes, respectively.

ID	$\alpha_{J2000.0}$	$\delta_{J2000.0}$	Period	Type	$<m_{F606W}>$	A_{F606W}	$<m_{F814W}>$	A_{F814W}	$<m_{V_0}>$	$<m_{I_0}>$
V1	0:43:01.7183	40:52:33.583	0.306	RRc	25.080	0.379	24.799	0.209	24.910	24.661
V2	0:43:01.8445	40:52:32.564	0.458	RRab	25.459	1.095	25.118	0.667	25.304	24.980
V3	0:43:03.9260	40:52:29.779	0.406	RRab	24.983	0.522	24.627[a]	-	-	-
V4	0:42:50.5077	40:52:29.038	0.584	RRab	24.940	0.682	24.530	0.475	24.794	24.392
V5	0:42:57.7187	40:52:28.670	0.310	RRc	25.422	0.460	25.082	-	-	-
V6	0:42:51.6067	40:52:27.570	0.399	RRc	24.846	0.451	24.465	0.287	24.703	24.326
V7	0:42:47.0945	40:52:27.376	0.690	RRab	25.182	1.073	24.151	-	-	-

[a] for one−filter RRLyr we have only one mean magnitude, thus we can not estimate the corresponding amplitude or Johnson-Cousin magnitudes, we can only indicate the Dolphot mean magnitude.

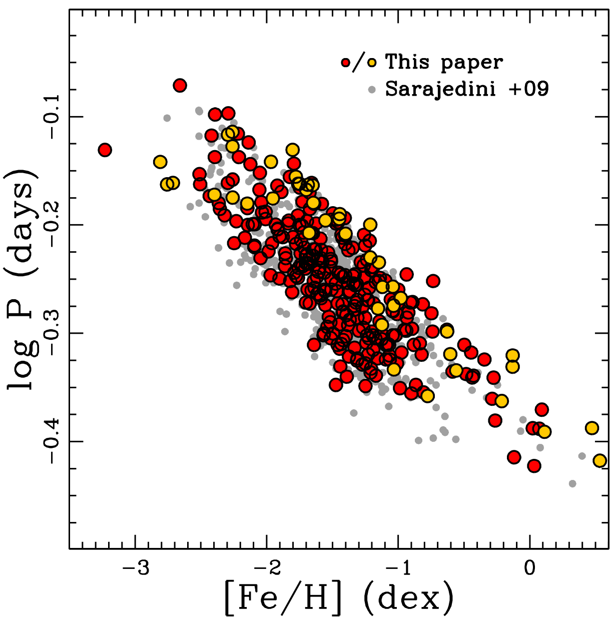

Fig. 5. The metallicity ([Fe/H]) −period (P) distribution for our sampled fundamental RRLyr. The colour code is the same used in Fig. 4. Undelying our observation those os Sarajedini et al. (2009) are shown as grey symbols.

3.2. The Horizontal Branch

The Horizontal Branch (HB) is almost invisible in our CMD, because it is sparsely populated and dominated by contamination from other populations, such as an extensive and broad RGB and a young BP of stars in the main sequence region. The only way to reliably identify the HB is using RRLyr. In Fig. 6a we show the CMD of the Horizontal Branch region for our *two-filters* RRLyr, for which we have light−curve weighted mean magnitudes and colours. The RRLyr define the HB and thus give us the opportunity to determine the mean distance modulus of the sample. To derive the distance modulus, we transformed mean m_{F606W} and m_{F814W} (columns 8 and 10 in Table 2) into Johnson−Cousins m_V and m_I (columns 12 and 13 in Table 2). We thus obtained a de−reddened V magnitude of the HB, $< V_0 > = 24.95 \pm 0.18$ mag. Then, assuming the average metallicity found above and using the M_V−[Fe/H] relationship (Carretta et al. 2000), we obtain a distance modulus of $\mu_0 = 24.33 \pm 0.21$ mag. The large uncertainty is due to both the large metallicity spread (see Fig. 5) and the large scatter on the HB (±0.5 mag), as seen in Fig. 6a.

In Fig. 6b, we show the luminosity histogram of our *two-filters* RRLyr and we compare it with that for field F1 from Sarajedini et al. (2009). The peak of our luminosity distribution is brighter than Sarajedini's by ∼0.16 mag. This could be due to the significantly different surface brightness of the two fields, which is ∼22 mag/arcsec^2 in our field and ∼25 mag/arcsec^2 in Sarajedini's. A brighter surface brightness implies more severe blending effects that can lead to brighter magnitudes for individual stars (e.g., Fiorentino et al. 2010b). However, the broad spread we find in m_{F606W} does not change using only the least blended[2] RRLyr in our sample. This suggests that this spread is not likely to be caused by photometric errors. The spread could be due to either the RRLyr being at a range of different distances and/or having a large range in metallicity. Note that in both cases differences in the evolutionary states may affect the RRLyr luminosity, which would further increase the final HB luminosity range. In Fig. 6a we show the effect of a metallicity range using the theoretical HB tracks for a range of metallicity at the mean distance modulus derived above. The metallicity spread inferred for the RRLyr is consistent with the large range derived from the periods and amplitudes in Fig. 4. However this does not account for the whole HB spread. In addition, a distance spread is also very likely because the M 32 field is mixed with M 31 population. Assuming the mean metallicity found above and moving the relative zero age HB locus to fit the brightest and the faintest RRLyr in Fig. 6a, we find a distance modulus of $24.33^{+0.47}_{-0.43}$ mag (or d = 734^{+178}_{-131} Kpc).

To determine how many, if any, of the RRLyr in our sample are likely to be associated with M 32, we need to look at their radial distribution from the centre of M 32.

4. The Cepheid variable stars

In our sample we have identified 7 variable stars (described in Table 3) with luminosities significantly higher than the HB, as shown in Fig. 6. These stars are at luminosities and colours consistent with both AC and P2C (Fiorentino et al. 2006; Di Criscienzo et al. 2007). The AC are core-He burning stars of intermediate age (∼1−6 Gyr old), with mass of 1−2$M_\odot$, and they cover a period range from a few hours to ∼2 days. The P2C are lower mass stars (≲0.8$M_\odot$) that just finished their core−He burning phase and come from the blue HB. They are very old (>10 Gyr) and typically have periods >1 day. Those with periods <3 days, are the so−called BL Hercules variable stars and they come from the *warm* part of the HB (e.g. Marconi et al. 2011).

The overlap in the period ranges of AC and P2C makes a proper distinction between them complicated. We have plotted them all in the Bailey diagram, see Fig. 4, where we see

---

[2] as defined by the DOLPHOT crowding parameter.

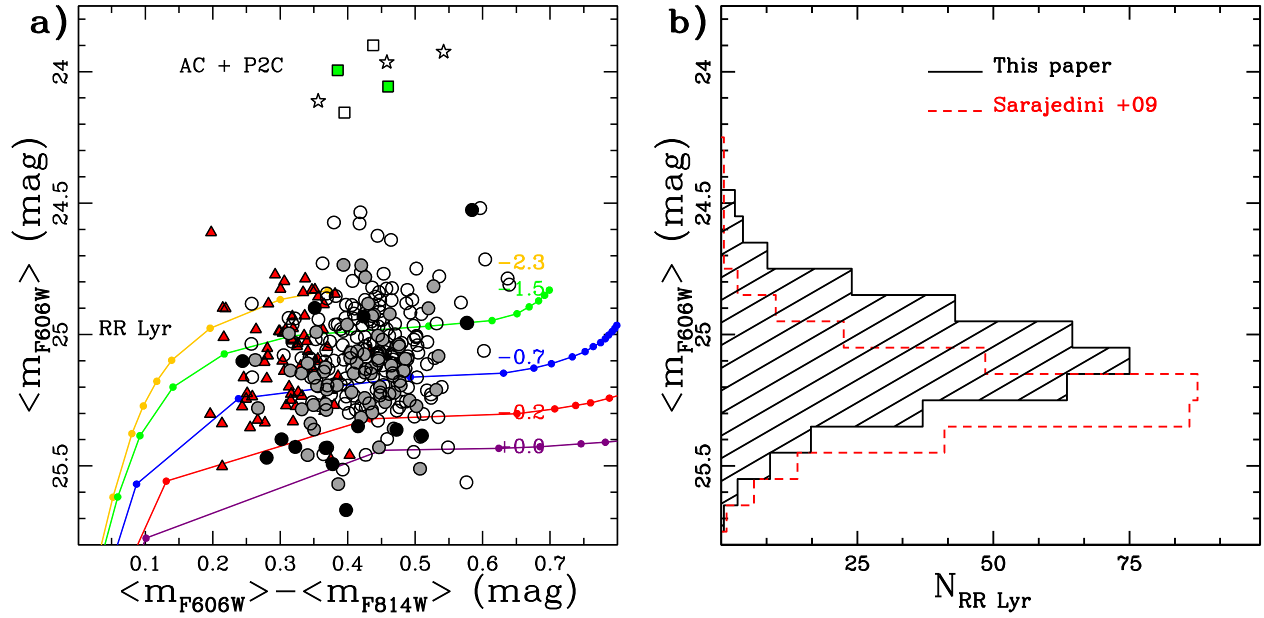

Fig. 6. **a):** the RRLyr region of the CMD, where only variable stars detected in two filters, with well defined colours and magnitudes, are shown. Red triangles are the same as in Fig. 2a, but the colouring of the F pulsators is determined by their metallicities, where empty circles are metal−poor ([Fe/H]≤ −1.5 dex), grey circles are metal−intermediate (−0.5 ≥[Fe/H]≥ −1.5 dex) and filled circles are metal−rich ([Fe/H]≥ −1 dex). AC and P2C are indicated with squares and stars, respectively. AC pulsating in first−overtone mode are highlighted with filled colour (green). The coloured lines are HB tracks from (Pietrinferni et al. 2004) for different metallicities, as labeled. **b):** the luminosity function for our 2-*filter* RRLyr sample (black solid line) compared with that found by Sarajedini et al. (2009) (red dashed line).

Table 3. The confirmed Cepheid variable stars. Same as in Table 2

ID	$\alpha_{J2000.0}$	$\delta_{J2000.0}$	Period	Type	$<m_{F606W}>$	A_{F606W}	$<m_{F814W}>$	A_{F814W}	$<m_{V_0}>$	$<m_{I_0}>$
C1	0:42:47.8102	40:50:53.238	1.78	P2C	23.964	0.782	23.506	0.579	23.839	23.368
C2	0:42:56.4848	40:51:06.308	0.70	AC−F	23.899	0.784	23.462	0.551	23.765	23.323
C3	0:42:57.9929	40:52:04.630	0.53	AC−FO	23.995	0.622	23.610	0.421	23.853	23.471
C4	0:42:54.1987	40:49:53.248	2.70	P2C	23.925	0.652	23.382	0.506	23.835	23.244
C5	0:43:02.8871	40:50:43.142	1.08	P2C	24.112	0.900	23.756	0.627	23.962	23.618
C6	0:42:51.8780	40:49:07.727	0.57	AC−FO	24.057	0.629	23.597	0.412	23.909	23.448
C7	0:43:02.5661	40:49:28.127	0.51	AC−F	24.156	0.815	23.761	0.547	24.017	23.622

that three of them occupy the region with periods >1 day, and the remaining four lie on the RRLyr Period−Amplitude relation. In Fig. 7 (lower panel) we plot the pulsation Instability Strip derived from theoretical models (Marconi et al. 2004) for AC, assuming the distance modulus derived in the previous section (μ_0=24.33). There is only one variable not within the instability strip, and this corresponds to the longest period, namely C4. To check that the Cepheids within the instability strip are genuine AC, we also use the colour information plotting them in the reddening−free Wesenheit plane, i.e. WES(V, V−I)=V−2.54E(V−I) see top panel of Fig. 7. In this plane the separation between these two classes of variables is very clear. The P2C follow a well established Period−Luminosity relation, whereas the AC follow a more spread out Period−Luminosity relation that depends on stellar mass. In Fig. 7 (top panel) we also show the theoretical Wesenheit relations (Fiorentino et al. 2007; Di Criscienzo et al. 2007) for both AC and P2C. Thus we can classify three Cepheids (C4, C6, C7) as P2C and the other four as AC (see Table 3).

We can constrain the masses for the four AC, using our theoretical approach (extensively described in Marconi et al. 2004; Caputo et al. 2005; Fiorentino et al. 2006) which allow us to simultaneously derive the mass and the pulsation mode of an AC using the pulsation properties. We use the well defined mass dependent Period−Magnitude−Amplitude relation, which is valid only for F pulsator, and the Period−Magnitude−Colour relations which are available for both F and FO pulsators. Applying these relations to our four AC we classify two of them F pulsators and the remaining FO pulsators (see Table 3) with masses in the range 1.2 – 1.9 $M_\odot$. Their masses indicate these stars come from a stellar population with ages between 1 and 4 Gyr old.

We notice that the distance modulus found from RRLyr agrees well with that from the P2C Wesenheit relation. The only point of concern is the low luminosity of the longest period P2C, C4. However mean luminosities and amplitudes could be affected by the small temporal coverage used to sample the full pulsation cycle for these relatively long period variable stars.

5. Radial distributions of Stellar Populations

The stellar populations of M 31 and M 32 are so similar and mixed, in our field, that the characteristics of M 32 can only be defined by looking for features that follow the strong concentration of stars towards the centre of M 32. This has to be done with extreme care, because the crowding properties of the images are also changing closer to the centre of M 32. We are mainly con-

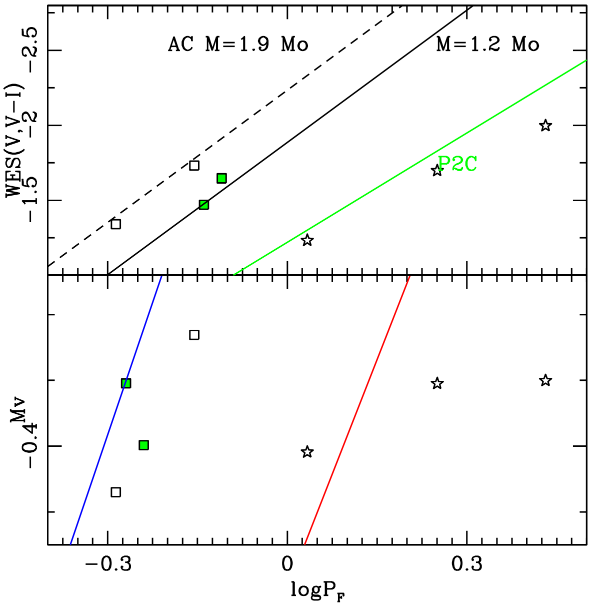

Fig. 7. *Bottom:* Anomalous Cepheids (squares) and Population II Cepheids (stars) in the M_V–period (P) plane. First–overtone AC have been highlighted with filled colour (green). It is not possible to make a clear classification between these two class of variables. We have plotted the cold (red) and the warm (blue) edges of the pulsation instability strip as derived by theoretical models (Fiorentino et al. 2006). *Top:* Wesenheit plane, where the separation between the Anomalous Cepheids and Population II Cepheids is clearer. The green solid line represents the relation for Population II Cepheids, and the black solid and dashed line represent the mass dependent Wesenheit relations for Anomalous Cepheids, with masses 1.2 $M_\odot$ and 1.9 $M_\odot$ respectively. The distance modulus assumed is 24.33, as we found from RRLyr.

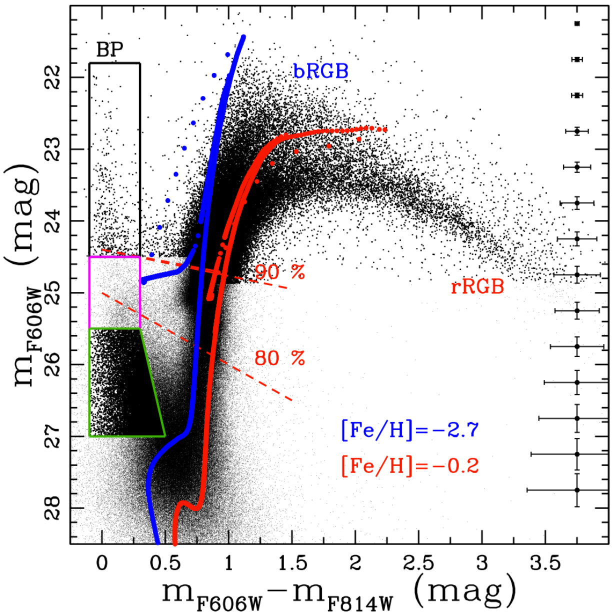

Fig. 8. The ACS/WFC CMD, for all the detected stars. The mean completeness levels (red dashed lines) and the photometric errors are shown. Over–plotted are 8 Gyr old reddened isochrones, from Pietrinferni et al. (2004) with [Fe/H]= −2.7 dex (blue) and −0.2 dex (red). Distance modulus and the reddening used are μ_0=24.33 and E(B−V)=0.08 mag. Isochrones and boxes have been used to select the populations. The blue (bRGB) and red RGB (rRGB) on either side of [Fe/H]= −0.2 dex isochrone and the blue plume (BP) which is separated into bright (black box), intemediate (magenta box) and faint (dark green box) components.

cerned to determine if there is a RRLyr population that can be reliably identified with M 32. To this end it is also useful to look at the radial distribution of other stellar populations that can be identified in our CMD.

In Fig. 8 we show the CMD for all the detected stars in our ACS/WFC field of view. The two over–plotted isochrones are 8 Gyr old, which is the mean age for the bulk of the stellar population (Monachesi et al. 2011). To look for spatial gradients over our field towards the centre of M 32, we select different stellar populations from the CMD, as follows:

i) the bright BP, which are young ≤500 Myr old main sequence stars;
ii) an intermediate BP, which includes a contribution from young main sequence stars (≤1 Gyr old) and also the blue HB;
iii) the faint BP, which is made up of main sequence stars ≤4 Gyr old;
iv) RRLyr;
v) the blue RGB, which is those stars with m_{F606W} ≤24.9 mag that lie on the RGB between the blue and the red isochrones and they should be mostly old metal–poor stars (-2.7≤[Fe/H]≤-0.2), but could also include younger (< 8 Gyr old) metal–rich stars ([Fe/H]≤-0.2);
vi) the red RGB, which is those stars with m_{F606W} ≤24.9 mag and on the red side of the red RGB and are all metal–rich RGB stars.

These populations have been chosen to trace different ages and metallicities in the CMD attempting to separate different contributions coming from M 31 and/or M 32. In fact, we do not expect that young stars with ages less than 0.5 Gyr belong to an elliptical galaxy such as M 32. On the other hand, we expect that the contribution to the metal–rich component, as the red RGB, is mostly coming from M 32, being almost invisible in other accurate HST CMDs of the disk/halo components of M 31 (e.g. Brown et al. 2006, and reference therein).

We expect that the completeness will vary along with the distance from the centre of M 32. For each selected population we have computed the completeness in annuli around M32, as defined in Fig 1. To account for the large colour baseline of our CMD, we computed the completeness for all the blue stars (V−I less than ~ 0.7 mag) and for all the red stars (V−I larger than ~ 0.7 mag) independently. As an example, at the luminosity of the RRLyr on the HB (m_{F606W} ~ 25.07 mag) the mean completeness for RRLyr is 57% in the inner annulus (r~ 1.3 arcmin), whereas it increases to 85% in the outer annulus (r~ 4.3 arcmin).

In Fig. 9, we show the number of stars per arcsec^2 of the selected stellar populations corrected for the completeness, as determined by artificial star tests. Four out of the six selected populations, i.e. the blue and red RGB, the intermediate BP and the RRLyr, increases going to the centre of M 32 defining the radial profile of the elliptical galaxy. On the contrary, the faint and bright BPs (top panel) show, if anything, a shallow opposite

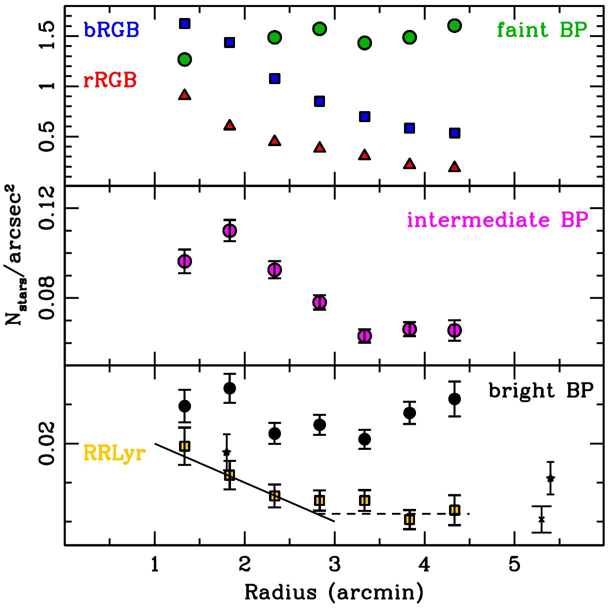

Fig. 9. The variation of the fraction of stars with the distance from the centre of M 32 for the populations selected from the CMD. The colour code is the same used in Fig. 8. The poissonian errorbars are plotted where they are larger than the symbols. Top panel, the bRGB, the rRGB and the faint BP have been plotted with circles, squares and stars, respectively. In the middle panel the intermediate BP distribution is plotted. The bottom panel shows the RRLyr and the bright BP radial distributions with squares and circles, respectively. The bright BP circles have been shifted of +0.01, to make the plot more clear. A comparison with previous RRLyr detections is also shown with stars (F1 and F2 Fiorentino et al. 2010b) and cross (F1 from Sarajedini et al. 2009). Solid and dashed lines represent the fit to M 32 and M 31 profiles, respectively.

trend, suggesting an association to M 31. Stars so young are a clear feature of the M 31 field from other ACS/WFC studies, and this suggests that all the young stars observed in our field are likely associated to M 31. However, the number statistics are low and it has been suggested by Monachesi et al. (2011) that there is a BP component in M 32 (with ages ≥1 Gyr). We do not confirm this finding, however it could easily be hidden in the huge contamination from M 31. We note that, among the BP components only the intermediate BP, which includes also stars from the HB, increases going towards the centre of M 32 (middle panel in Fig. 9) then supporting the presence of the HB in M 32. If there were young stars in M 32 then also the other BP components should show the same signature, but they do not.

Finally, the RRLyr distribution found in the present study shows an increasing trend towards the centre of M 32 and confirms previous results (Alonso-García et al. 2004; Fiorentino et al. 2010b). In Fig. 9 we also showed the RRLyr detections found from Sarajedini et al. (2009) and Fiorentino et al. (2010b), which are in very good agreement with the RRLyr radial profile found in this paper. Our previous RRLyr detections, two points from Fiorentino et al. (2010b), were uncertain because of their large poissonian errors due to the very small FoV (30x30 arcsec) of ACS/HRC. Our new detection of 416 RRLyr and their spatial variation over the 3.3′x3.3′ ACS/WFC field of view is the strongest evidence obtained so far for an ancient population in M 32.

We also notice that the RRLyr distribution is quite flat going from outside to the centre of M 32 up to about 3 arcmin, suggesting that what we are observing for radii larger than 3 arcmin is a high background from M 31. Something similar can be seen also in the intermediate BP distribution supporting the idea of the strong M 31 background.

We can attempt an estimation of the fraction of the RRLyr that belong to M 32 by assuming that the RRLyr outside ~3 arcmin from the centre of M 32 represent the M 31 background (N_{stars}/arcsec^{2}=0.011, dashed line in Fig. 9). Then, we can fit a slope to the remaining observations ($r \leq 3$ arcmin), N_{stars}/arcsec^{2}=0.025−0.005*r (solid line in Fig. 9). The total number of stars whithin 3 arcmin from the centre to M 32 is 327 RRLyr, which includes the background from M 31. Then we can estimate the number of RRLyr inside the 3 arcmin, subtracting the contribution expected from the background of M 31. At least ∼ 83 RRLyr could to be associated to M 32.

6. Conclusions

The radial density of RRLyr in our HST/WFC sample clearly increases towards the centre of M 32. This convincingly shows that we have identified an ancient stellar population of at least 83 RRLyr associated to M 32. These new RRLyr detections are in agreement with our previous results (Fiorentino et al. 2010b), which is actually a bit lucky given the statistics of the small field of view of HST/HRC.

The same trend towards the centre of M 32 is also followed by the other stellar components. Such as the blue and the red component of the RGB. This suggests that M 32 contains both a moderately metal−poor (-2.7≤[Fe/H]≤-0.2) and a metal−rich ([Fe/H]≥-0.2) stellar population.

On the other hand, the bright and the faint blue plume of young main sequence stars (≤ 4 Gyr old) has a more smooth distribution suggesting that it is associated exclusively with the M 31 background. This result suggests that the 4 AC, with masses from 1.2 to 1.9 $M_{\odot}$, found in our analysis are likely to be associated to M 31.

We find compelling evidence for a large spread in the metallicities of the RRLyr in our sample. They span -2.4≤[Fe/H]≤0 dex with a mean metallicity of <[Fe/H]>∼ -1.44±0.55 dex.

The RRLyr in this study are classified as Oosterhoff type I, in agreement with recent results (Brown et al. 2004; Jeffery et al. 2011) for RRLyr observed in M 31. The properties of our RRLyr sample resemble those of the stream of M 31. This could suggest that M 32 could have contributed to the M 31 stream with its old stellar population, or that the stream dominates M 31 at the position of M 32.

Acknowledgments

We thank A. Dolphin and D. Weisz for their technical support running DOLPHOT on many WFC/ACS images simultaneously. We are grateful to A. Mucciarelli for his help in calculating the reddening map of our WFC/ACS field. We thank S. Cassisi, M. Di Criscienzo, G. Greco, M. Bellazzini and G. Bono for useful discussions. GF particularly thanks R. Merighi his technical support. The authors acknowledge an anonymous referee for his/her suggestions that improved the content and the readability of the manuscript. GF and ET have been supported by a NWO−VICI grant and GF by the INAF fellowship 2009 grant. ET thanks the hospitality of Observatiore de la Côte d’Azur.

References

Alcock, C. et al. 2000, AJ, 119, 2194
Alonso-García, J., Mateo, M., & Worthey, G. 2004, AJ, 127, 868
Bedin, L. R., Cassisi, S., Castelli, F., et al. 2005, MNRAS, 357, 1038
Brown, T. M., Ferguson, H. C., Smith, E., et al. 2004, AJ, 127, 2738
Brown, T. M., Smith, E., Ferguson, H. C., et al. 2006, ApJ, 652, 323
Caputo, F., Bono, G., Fiorentino, G., Marconi, M., & Musella, I. 2005, ApJ, 629, 1021
Carretta, E., Gratton, R. G., Clementini, G., & Fusi Pecci, F. 2000, ApJ, 533, 215
Clement, C. M. 2000, in Astronomical Society of the Pacific Conference Series, Vol. 203, IAU Colloq. 176: The Impact of Large-Scale Surveys on Pulsating Star Research, ed. L. Szabados & D. Kurtz, 266
Clementini, G., Contreras, R., Federici, L., et al. 2009, ApJ, 704, L103
Coelho, P., Mendes de Oliveira, C., & Fernandes, R. C. 2009, MNRAS, 396, 624
Di Criscienzo, M., Caputo, F., Marconi, M., & Cassisi, S. 2007, A&A, 471, 893
Dolphin, A. E. 2000a, PASP, 112, 1397
Dolphin, A. E. 2000b, PASP, 112, 1383
Dolphin, A. E., Saha, A., Olszewski, E. W., et al. 2004, AJ, 127, 875
Fiorentino, G., Contreras Ramos, R., Clementini, G., et al. 2010a, ApJ, 711, 808
Fiorentino, G., Limongi, M., Caputo, F., & Marconi, M. 2006, A&A, 460, 155
Fiorentino, G., Marconi, M., Musella, I., & Caputo, F. 2007, A&A, 476, 863
Fiorentino, G., Monachesi, A., Trager, S. C., et al. 2010b, ApJ, 708, 817
Grillmair, C. J. et al. 1996, AJ, 112, 1975
Jeffery, E. J., Smith, E., Brown, T. M., et al. 2011, AJ, 141, 171
Marconi, M., Bono, G., Caputo, F., et al. 2011, ApJ, 738, 111
Marconi, M., Fiorentino, G., & Caputo, F. 2004, A&A, 417, 1101
Monachesi, A., Trager, S. C., Lauer, T. R., et al. 2011, ApJ, 727, 55
Pietrinferni, A., Cassisi, S., Salaris, M., & Castelli, F. 2004, ApJ, 612, 168
Piotto, G., Zoccali, M., King, I. R., et al. 1999, AJ, 118, 1727
Pritchet, C. J. & van den Bergh, S. 1987, ApJ, 316, 517
Rejkuba, M., Harris, W. E., Greggio, L., & Harris, G. L. H. 2011, A&A, 526, A123+
Renzini, A. 2006, ARA&A, 44, 141
Rose, J. A. 1994, AJ, 107, 206
Sarajedini, A., Mancone, C. L., Lauer, T. R., et al. 2009, AJ, 138, 184
Sirianni, M. et al. 2005, PASP, 117, 1049
Trager, S. C., Faber, S. M., Worthey, G., & González, J. J. 2000, AJ, 119, 1645